PROCEEDINGS : CAMME - 1996
@NML JAMSHEDPUR, PP. 222-233

Mathematical modelling of peritectic transformation in binary systems

A. DAS. I. MANNA and S. K. PABI*

** Department of Metallurgical and Materials Engineering, Indian Institute of Technology, Kharagpur 721 302, India*

ABSTRACT

A simple diffusional analysis of peritectic transformation based on the linearized concentration gradient approximation and a rigorous numerical model of the peritectic transformation as well as the solid state homogenization process following liquid depletion has been presented. The overall and interface mass balance equations are utilized to calculate the rate of movement of the interfaces in the finite geometry. The predictions of the present models, show a better agreement with the experimentally determined kinetic data from the Cd-Ag and Pd-Bi systems as compared to those by the earlier proposed models based on quasi-static interface or time-invariant or Laplacian concentration profiles. However, the computed kinetics differ from the observed rates of transformation at a later stage (~50% transformation), perhaps, due to the deviation from the idealized cell configuration considered in the calculations.

INTRODUCTION

Transformation of a binary two phase aggregate comprising a solid and liquid phase into a new solid on cooling is termed as peritectic change[1]. Peritectic change may occur through two distinct stages[2]. In the first stage, the liquid reacts with the primary solid (β) to form the secondary solid (α) that grows along the periphery of β. This stage is known as the peritectic reaction. When β is completely enveloped by α, the reactant phases (β and liquid) lose contact with each other and compel the peritectic change to proceed by solute transport through the α-envelope. This second stage (i.e. peritectic transformation) seldom reaches completion and results in microsegregation. Peritectic transformation has so far been utilized mainly for grain refinement in some Al-based alloys[3-7] and liquid route processing of YBCO-superconductors[8-13]. Though peritectic change is a common invariant reaction in the metallic/ceramic systems, a comprehensive understanding of the

transformation mechanism and kinetics is still lacking. An extremely slow reaction kinetics and presence of liquid in the microstructure further complicates experimental investigation. Moreover, a distinction between the α formed through peritectic transformation and through direct solidification of the remnant liquid often becomes too difficult in the microstructure. As an alternative, mathematical modeling has been attempted in the past to elucidate the kinetics. From the diffusion couple experiments, Titchner and Spittle[14] have proposed that the transformation is governed by diffusion through α - layer, the degree of thickening of which is governed by a power law: $w=At^n$. The time exponent 'n' varies from 0.36-0.57 depending on the alloy system. St .Jhon and Hogan[15] have arrived at a similar expression with n=0.5. Maxwell and Hellawell[6] have used Laplacian approximation to represent the solute distribution profiles in α and liquid phases, and solved mass balance equations to calculate the rate of displacement of the concerned interfaces assuming nearly invariant α-β interface position. On the other hand, St. John[16] has shown that α-layer formation prior to peritectic transformation occurs through direct solidification rathe than through peritectic reaction for most peritectic systems. Under these circumstances, a cored profile in β and α are quite likely. Recenly, Lopez[17] has presented a more detailed analytical solution that allows a stationary cored profile to exist in β. Since solution of unsteady state diffusion equations in moving phase fields is difficult, all these analytical models assume a quasi-stationary interface position during the transformation. However, in case of precipitate dissolution it has been demonstrated that quasi-static interface approximation significantly overestimates the kinetics[18]. Moreover, these models ignore impingement of diffusion fields around adjacent β particles, which restricts the applicability of the solution to only the dilute alloys with isolated or very widely spaced β particles.

Chuang et al.[19] have proposed a numerical model that couples unsteady state diffusion equations with material balance at the interfaces of the Fe-Fe_3C system, to predict the interface positions with time. Fredriksson and Nylen[20] have combined material balance equations on either side of α with an overall mass balance, which was subsequently solved numerically to generale the α thickening rate. These numerical models, however, overlooked the time modulation of diffusion field widths in course of the transformation. Besides, none of the models on peritectic transformation proposed so far has been systematically tested against the relevant experimental data.

This paper presents an analytical as well as more rigorous numerical model for peritectic transformation. The results predicted by the present models have been compared with experimental kinetic data from the Cd-Ag and Pb-Bi systems.

THE MATHEMATICAL MODEL

Fig. 1 presents a schematic binary phase diagram showing a peritectic change: liquid + β —> α. Let us consider an alloy of initial composition C_0 is cooled through the peritectic temperature (T_p) to an isothermal transformation temperture T_1 ($<T_p$) and held for isothermal peritectic change. Peritectic transformation kinetics at T_1 may be represented by an idealized spherical transformation cell (Fig. 2a) of radius $R_i = [N_\beta(3/4\pi)]^{1/3}$, where N_β is the number of β nuclei (equispaced spheres) per unit volume. At T_p, the cell comprises β of radius S_{1p} inside a liquid pool of outer radius R_i. Subsequent cooling to T_1 produces a very thin concentric layer of α of outer radius S_{2p} and thickness (S_{2p}-S_{1p}) around the pro-peritectic β (Fig. 2a). It may be noted that growth of α during the isothermal peritectic transformation at T_1 is accompanied by migration of both the α-β interface located at S_1 and α-liquid interface at S_2. The concerned interfacial concentration values for this diffusion controlled transformation may be obtained from Fig. 1.

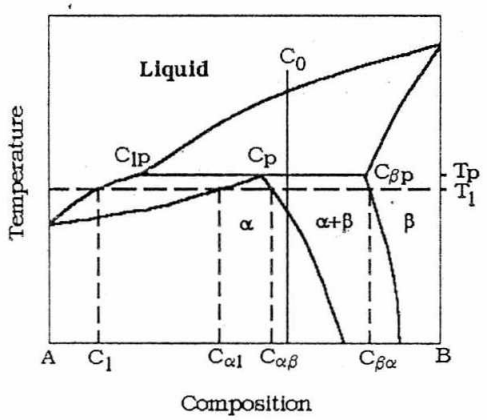

Fig. 1 : A Schematic binary phase diagram defining the concentration terms for a petitectic change

S_{1p} at T_p may be obtained by an overall mass balance as :

$$\dot{U}C_\beta r^2dr + C_{lp}r^2dr + \ = C0r2dr \qquad \ldots 1$$

S_{2p} at the onset of isothermal transformation may be determined through a similar exercise as follows :

$$\int_0^{S_{1p}} C_\beta r^2dr + \int_{S_{1p}}^{S_{2p}} C_\alpha r^2dr + \int_{S_{2p}}^{R_i} C_l r^2dr = \int_0^{R_i} C_0 r^2dr \qquad \ldots 2$$

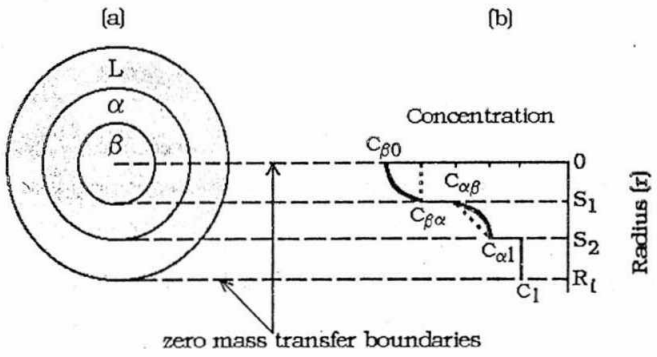

Fig. 2 : (a) A representative peritectic transformation cell, and (b) corresponding concentration profiles existing in the participating phases

It may be noted that S_{1p} and S_{2p} represent the respective positions of the β-α and α-liquid interfaces at T_1 for t = 0. Concentration profiles in the solid phases during the course of transformation at T_1 (t>0) are given by the unsteady state diffusion field equations :

$$\frac{\partial C}{\partial t} = \frac{1}{r}\frac{\partial}{\partial r}\left(r^2 D \frac{\partial C}{\partial r}\right) \qquad \ldots 3$$

while the liquid is assumed to maintain a homogeneous composition C_l due to instantaneous mixing.

The β-α interface location at a given t may be obtained from the mass balance condition across the concerned interface :

$$\left(C_{\beta\alpha} - C_{\alpha\beta}\right)\frac{dS_1}{dt} = -D_\beta\left[\frac{dC}{dr}\right]_{r=S_1} + D_\alpha\left[\frac{dC}{dr}\right]_{r=S_1} \qquad \ldots 4$$

On the other hand, the α-liquid interface location is solved through the following overall mass balance equation :

$$\int_0^{S_1} C_\beta r^2 dr + \int_{S_1}^{S_2} C_\alpha r^2 dr + \int_{S_2}^{R_i} C_l r^2 dr = \int_0^{Ri} C_0 r^2 dr . \qquad \ldots 5$$

Solutions of equations (3-5) yields the concentration gradients and the interface positions during the course of isothermal peritectic transformation at T_1.

ANALYTICAL SOLUTION

Here, the β phase is assumed to be homogeneous and following Zener's approach of linearized concentration gradient[21], composition gradient at T_1 inside the α-phase in the transformation cell is assumed to be linear in the spatial variable r (dotted lines in Fig. 2b). Accordingly, equation (1) yields,

$$S_{1p} = R_i [(C_0 - C_{1p}) / (C_{\beta p} - C_{1p})]^{1/3} \quad \ldots 6$$

where, $C_{\beta p}$ and C_{1p} represent the respective concentration values of the β and liquid phases in contact with each other. Similarly, S_{2p} may be determined through equation (2) as :

$$S_{2p} = \left[\frac{R_i^3 (C_0 - C_l) + S_{1p}^3 \left[\frac{1}{2}(C_{\alpha\beta} + C_{\alpha l}) - C_{\beta\alpha} \right]}{\frac{1}{2}(C_{\alpha\beta} + C_{\alpha l}) - C_l} \right]^{1/3} \quad \ldots 7$$

where, $C_{\alpha\beta}$ and $C_{\alpha l}$ are the concentrations of the α-phase at the α-β and α-liquid interfaces at T_1, respectively. Furthermore, $C_{\beta\alpha}$ and C_1 are the respective concentration terms of the β and liquid phases at T_1. Similar mass balance is applicable throughout the isothermal transformation, and hence, the location of the α-liquid interface at a given t may be represented as follows :

$$S_2 = \left(\frac{AR_i^3 + BS_1^3}{K} \right)^{1/3} \quad \ldots 8$$

where, $A = (C_0 - C_1)$, $B = [0.5(C_{\alpha\beta} + C_{al}) - C_{\beta\alpha}]$, and $K = [0.5(C_{\alpha\beta} + C_{\alpha l}) - C_1]$

The β-α interface mass balance equation (4) may be rearranged substituting S_2 from equation (8) as,

$$\int_{S_{1p}}^{S_1} \left[\left(\frac{A}{K} \right)^{1/3} R_i \left\{ 1 + \frac{B}{A} \left(\frac{S_1}{R_i} \right)^3 \right\}^{1/3} - S_1 \right] dS_1 = D_\alpha \left(\frac{C_{\alpha l} - C_{\alpha\beta}}{C_{\beta\alpha} - C_{\alpha\beta}} \right) \int_0^t dt \quad \ldots 9$$

where, D_α is the interdiffusion coefficient in α.

For $\{(B/A)\ (S_1/R_i)^3\} << 1$, binomial expansion of the term in braces in equation (9) (neglecting $(S_1/R_i)^9$ and higher order terms) and subsequent integration leads to :

$$\left[S_1 + \frac{1}{12}\left(\frac{B}{A}\right)\left(\frac{S_1^4}{R_i^3}\right) - \frac{1}{63}\left(\frac{B}{A}\right)^2\left(\frac{S_1^7}{R_i^6}\right) - \frac{S_1^2}{2}\left(\frac{K}{A}\right)^{1/3}\frac{1}{R_i} \right]_{S_{1p}}^{S_1} = \frac{D_\alpha}{R_i}\left(\frac{K}{A}\right)^{1/3}\left(\frac{C_{\alpha l} - C_{\alpha\beta}}{C_{\beta\alpha} - C_{\alpha\beta}}\right) t \quad \ldots 10$$

Equation (10) may be used incorporating the values of the constants A, B, K, and S_{1p}) to determine the β-α interface position at a given t during the isothermal transformation. Subsequently, the value of S_1 is substituted in equation (8) to calculate S_2 at that instant.

NUMERICAL SOLUTION

Unlike the analytical solution which assumes a homogeneous β, a cored concentration profile inside the β-phase (firm line in Fig. 2b) formed on cooling a liquid of composition C_0 to the peritectic temperature (T_p) may be described by Scheil's equation as :

$$C_\beta = K_1 C_0 [1 - (r_\beta / R_i)^3]^{K1-1}] \quad \ldots 11$$

Therefore, β-phase radius (S_{1p}) at the onset of reaction (at T_p) may be obtained as :

$$S_{1p} = R_i \, [1-(C_{\beta p} / K_1 C_0)_{1/K1} \,]^{1/3} \qquad \ldots 12$$

where K_1 is the equilibrium solute distribution coefficient at the β-liquid interface at T_p. On further cooling to the transformation temperature $T_1 (<T_p)$, α is assumed to form through solidification of liquid of concentration C_{1p} at T_p, in conformity with St. John's[16] observation. Again a segregation profile is approximated in α (firm line in Fig. 2b) so that composition in α may be represented as :

$$C\alpha = K_2 C_{1p} [1-(r_\beta^3 - S_{1p}^3) / (R_i^3 - S_{1p}^3)]^{K2-1} \qquad \ldots 13$$

The outer radius of α, (S_{2p}) when a fully envelopes β i.e. at the onset of the transformation (t = 0), may be calculated as :

$$S_{2p} = [S_{1p}^3 + \{R_i^3 - S_{1p}^3\} \{1-(C_{\alpha l} / K_2 C_{1p})^{1/K2-1}\}]^{1/3} \qquad \ldots 14$$

where K_2 is the solute distribution coefficient in β and $C_{\alpha l}$ is the concentration in the α-layer at the α-liquid interfae.

Numerical solution is obtained for the coupled equations (3) to (5). The chang in phase thickness in course of transformation has been taken care of by applying the Murray and Landis[22] variables grid space transformation. The mathematical treatment is somewhat similar to that for precipitate dissolution by Tanzilli and Hackell[23].

The rate of change of concentration at a point 'n' which may be represented as a constant fraction of the instantaneous phase thickness may be given by :

$$\frac{dC_n}{dt} = \frac{\delta C_n}{\delta r_n} \left(\frac{dr_n}{dt} \right) + \frac{\delta C_n}{\delta t} \qquad \ldots 15$$

Incorporating the diffusion field equation for a phase one may write,

$$\frac{dC_n}{dt} = \frac{\delta C_n}{\delta r_n} \left(\frac{dr_n}{dt} \right) + D\left[\frac{\delta^2 C_n}{\delta r^2_n} + \frac{2}{r_n} \frac{\delta C_n}{\delta r_n} \right] \qquad \ldots 16$$

for concentration independent D.

β phase :

The n-th grid point is defined as $r_n = P.S_1$ where A is a constant. Accordingly, equation (16) transforms to :

β phase :

$$\frac{dC_n^{\beta}}{dt} = \frac{r_n}{S_1}\frac{\delta C_n}{\delta r_n}\frac{dS_1}{dt} + D\beta\left[\frac{\delta^2 C_n}{\delta r_n^2} + \frac{2}{r_n}\frac{\delta C_n}{\delta r_n}\right] \quad \ldots 17$$

Here, the n-th grid point may be expressed as,

$r_n = S_1 + Q[S_2 - S_1]$ where Q is another constant

The diffusion field equation for α becomes,

$$\frac{dC_n^{\alpha}}{dt} = \frac{\partial C_n}{\partial r_n}\left[\frac{dS_1}{dt} + \frac{r_n - S_1}{S_2 - S_1}\left(\frac{dS_2}{dt} - \frac{dS_1}{dt}\right)\right] + D_{\alpha}\left[\frac{\partial^2 C_n}{\partial r_n^2} + \frac{2}{r_n}\frac{\partial C_n}{\partial r_n}\right] \quad \ldots 18$$

Equations (17-18) and (4) are solved through finite difference to yield the instantaneous concentration profiles in β, α and the concerned β-α interface position. On the other hand, equation (5) is solved through numerical integration utilizing Simpson's formula to determine the corresponding a-liquid interface location.

TWO PHASE HOMOGENIZATION

When S_2 reaches $0.999R_i$, liquid is assumed to be depleted and transformation proceeds further by β-α homogenization. Concentration inside the β-phase may still be obtained through equation(17). Diffusion field equation applicable to the α-phase transforms to :

$$\frac{dC_n^{\alpha}}{dt} = \frac{\partial C_n}{\partial r_n}\frac{R_i - r_n}{R_i - S_1}\frac{dS_1}{dt} + D_{\alpha}\left[\frac{\partial^2 C_n}{\partial r_n^2} + \frac{2}{r_n}\frac{\partial C_n}{\partial r_n}\right] \quad \ldots 19$$

Due to impingement of diffusion fields, concentration at the α-outer boundary now changes with time. Accordingly, a virtual grid is constructed outside this zero mass transfer boundary to calculate the concentration value at R_i at a particular time sequence in the finite difference scheme. The β-α boundary position is determined through equation(4). β-phase is assumed to be depleted when S_1 reaches $0.001R_i$ and calculations are terminated.

RESULTS AND DISCUSSIONS

Cd-Ag is selected as a model system for validation of the results predicted by the analytical model. It is known that a cored composition profile is anticipated in the secondary phase enveloping the pro-peritectic phase, if the former forms essentially through a direct/isomorphous solidification from the remnant liquid. Since the present analytical model envisages a linearized gradient in α during peritectic transformation, presence of coring may adversely affect the accuracy of the results. Therefore, it is fortunate that α

forms primarily through peritectic reaction in the Cd-Ag system[15] and rules out the possibility of significant coring in it. On the other hand, it has been observed earlier that α in Pb-Bi system have the tendency to form through solidification from the melt[24]. Moreover, coring in Pb-rich β-phase may not be unusual. As a consequence, isothermal kinetic data on peritectic transformation in Pb-Bi system[25] has been utilized to validate the numerical model which assigns cored profiles in the solid phases.

Fig. 3 compares the predictions of the analytical model with experimental kinetic data from the Cd-5at.% Ag alloy. The plot reveals remarkable agreement betwenen experimental and estimated normalized β radius at the initial stage up to $D_\alpha t/R_i^2 = 0.5$. Similarly, Fig. 4 compares the predictions of the numerical model with experimentally determined β dissolution data from the Pb-33.3 wt.% Bi[25] alloy. Parametric values used for the calculations are presented in Table 1. Due to the non-availability of volume diffusion coefficients in the α phases, diffusivities were approximated to be in the order of 10^{-12} m^2/s, which gives a better matching for all the models considered. The predicted kinetics have deviated from the experimental data beyond about 50% dissolution of β.

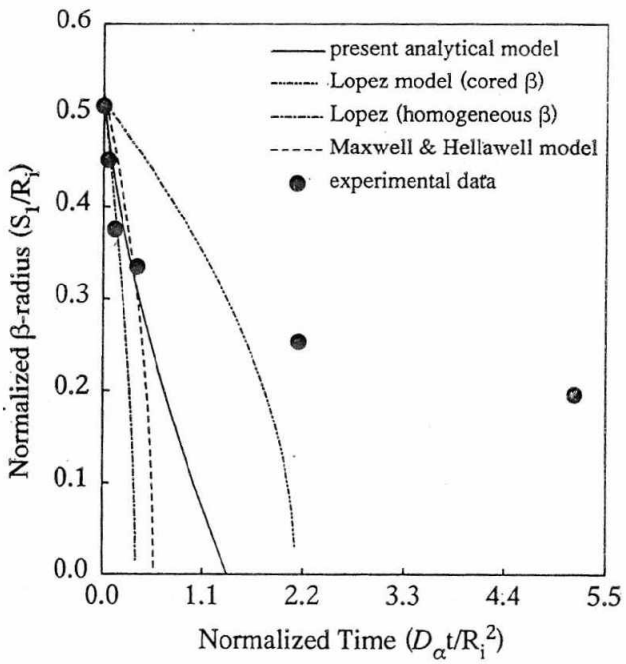

Fig. 3 : Comparison of peritectic transformation kinetics in a Cd-5at.% Ag alloy isothermally transformed at 608K

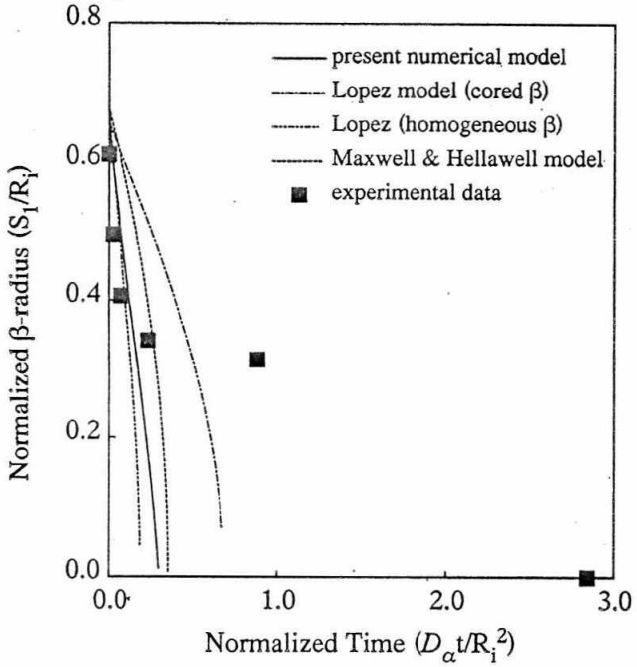

Fig. 4 : Comparison of peritectic transformation kinetics in a Pb-33.3 wt.% Bi alloy isothermally transformed at 443K.

Table 1

Input parameters for the calculation of peritectic transformation kinetics.

Phase Dig.	C_0 (at. fr.B)	T_1 (K)	R_i (m)	K_1	K_2	Eq. composn. (at. fr.B)				D (m^2/s)
						$C_{\beta\alpha}$	$C_{\alpha\beta}$	$C_{\alpha l}$	$C_{\alpha l}$	
Cd-Ag	0.05	608	1.2×10^{-4}	0.135	2.692	0.193	0.070	0.040	0.016	10^{-12}
Pb-Bi	0.33	443	10^{-3}	0.795	1.333	0.216	0.285	0.330	0.443	10^{-12}

For a comparison of our results with the existing mathematical models, the predictions from the Lopez[17] and Maxwell and Hellawell[6] models have also been included in Figs. 3 and 4. From Fig. 3, it is apparent that a satisfactory match is obtained only up to $D_\alpha t/R_i^2 = 0.2$. Similar results are also observed in Fig. 4. Assumption of linear gradient in the Lopez model has resulted in a poor agreement with experimental data beyond about 30/40% dissolution. When the Lopez model assumes a cored profile in β the predicted results deviate from the experimental kinetics fom the onset of transformation. Similar deviations are

observed for predictions from Maxwell and Hellwell model. Both the models by Lopez and Maxwell and Hellawell fail to effectively simulate the gradual slowing down of the transformation kinetics. From diffusional considerations, solute atoms have to migrate through a progressively thickening α-layer. As diffusion through α is the rate controlling step, transformation kinetics is expected to retard significantly towards the end. The Laplacian profile approximation in Maxwell and Hellawell model gives suficient convergence only in the beginning of the transformation when the impingement of the diffusion fields can be ignored. On the other hand, the approximation of quasi-static interface position in Lopez model neglects the changes in the local concentration gradient due to the movement of the interface. Since the interface velocity or transformation rate is decided by the local gradient at the interfaces[18], Lopez model tends to overestimate the transformation rate. The assumption of time invariant concentration profile introduces further error when the Lopez model considers a cored profile in β. The model does not alloy β to homogenize during the progress of transformation and therefore provides a source of virtual solute flux from the dissolving β to the β-α boundary. As a consequence, the results predicted by his model underestimates the experimental kinetics right from the onset of the transformation. The present analyses, therefore, appears to be superior in predicting the kinetics of peritectic transformation compared to the earlier proposed models based on quasi-static interface and Laplaian or time invariant composition profile approximation.

The deviation beyond $D_\alpha t/R_i^2 = 0.5$ arises possibly due to the departure of the transformation cell from the ideal geometry (cf. Fig. 2) at the later stage of the experiments caused by : (a) early impingement of the diffusional fields and (b) displacement of the entrapped liquid leading to the formation of voids. Fig. 5 presents a typical microstructure from the Cd-5at.%Ag alloy isothermally transformed at 608 K for 15 min. Though the connectivity of the liquid is still observed in the microstructure, early impingement of diffusional fields around some of the closely spaced β-particles are distinct. Fig. 6 represents a typical microstructure from the same specimen after 2h. The formation of a void or cavity (area 'A') in the isolated liquid area which could otherwise solidify into a fine two-phase structure (like in area 'C') is evident. This has markedly altered the idealized geometry considered in the models (cf. Fig. 2). Moreover, β particles existing in microstructure differ in shape and size which may affect the average dissolution rate at a later stage. As a consequence , the transformation kinetics are significantly retarded as compared to that in the early part of the transformation. Nevertheless, the gradual retardation of the kinetics with the progress of the transformation is qualitatively corroborated by the predictions of the present model.

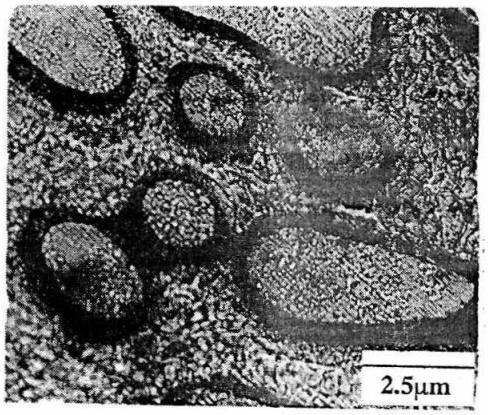

Fig. 5: Quenched microstructure of a Cd-4at.% Ag alloy, following isothermal transformation at 603K for 15 min. β appears white and α ppears dark. The liquid phase have solidified into a fine two-phase structure.

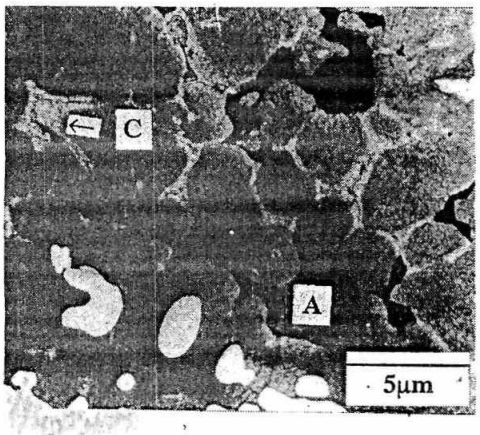

Fig. 6: Quenched microstructure of Cd-5at.% Ag alloy after isothermal holding at 608K for 2h illustrating cavity (marked 'A') formation due to expulsion of the liquid which otherwise solidifies as the grey region (marked 'A').

CONCLUSION

An analytical model on the kinetics of peritectic transformation based on the linearized concentration gradient approximation has been presented and validated through a suitable comparison with the relevant experimental data from the Cd-Ag system. Moreover, a rigorous numerical model on the kinetics of finite extent peritectic transformation has also been presented utilizing overall and interface mass balance equations and extended to the solid state homogenization process following liquid consumption. Predictions from the numerical model have been compared with expermental results from Pb-Bi system. The predictions by the present models show a better agreement with the experimental results than those by the earlier proposed models based on quasi-static interface and time invarient or Laplacian concentration profile approximaton. The observed reaction rates, however, show divergence from the rates computed through the present model at the later stages of transformation ($D_\alpha t/R_i^2 > 0.5$ or 50% β dissolution) possibly due to the deviation from the idealized geometry arising out of liquid entrapment and/or void formation in addition to the wide variation in size and shape of the properitectic phase.

REFERENCES

[1] A. D. Pelton, in: Phase Transformations in Materials, *Materials Science and Technology,* R. W. Cahn, P. Haasen and E. J. Kramer (Eds.), vol. 5, p. 29, VCH Verlagsgesellschaft GmbH, Weinheim, FRG (1991).

[2] H. W. Kerr, J. Cisse and G. F. Bolling, *Acta Metall.* 22 (1974) 677.

[3] F. A. Crosley and L. F. Mondolfo, *Trans. Met. Soc.* AIME 191 (1951)1143.

[4] A. Cibula, *J. Inst. Metals* 76 (1949) 321.

[5] I. Maxwell and A. Hellawell, *Trans. Met. Soc.* AIME 3 (1972) 1487.

[6] I. Maxwell and A. Hellawell, *Acta Met.* 23 (1975) 901.

[7] P. C. VanWiggen and W. H. M. Alsem, *Light Metals, Proc.* TMS Annual Meeting Warrendale, Pennsylvania (1993) p.763.

[8] K. Sawano, M. Morita, K. Miyamoto, K. Doi, A. Hayashi and M. Murakami, *J. Ceramic Soc. Jpn.* 97 (1989) 1028.

[9] A. Goyal, P. D. Funkenbusch, D. M. Kroger and S. J. Burns, *Physica C:Superconductivity* 182 (1991) 203.

[10] Y. A. Jee, S. J. L. Kang, J. H. Suh and D. Y. Yoon, *J. Amer. Ceramic Soc.* 76 (1993)2701.

[11] N. Pellerin, P. Odier, P. Simon and D. Chateigner, *Physica C: Superconductivity* 228 (1994) 351.

[12] C. J. Kim, K. B. Kim and G. W. Hong, *Materials Letters* 21 (1994)9.

[13] M. Ullrich and H. C. Freyhardt, *Physica C: Superconductivity* 235-240 (1994) 455.

[14] A. P. Titchner and J. A. Spittle, *Metal Sci.*, 8 (1974) 112.

[15] D. H.St John, and L. M. Hogan, *Acta Metall.* 25 (1977)77.

[16] D. H. St. John, *Acta Metall.* 38 * 1990) 631.

[17] H. F. Lopez, *Acta Metall.*, Mater. 39 (1991) 1543.

[18] S. K. Pabi, Acta Met. 27 (1979) 1693.

[19] Y. K. Chuang, D. Reinisch and K. Schwerdtfeger, *Metall. Trans.* 61A (1975)235.

[20] H. Fredriksson and T. Nylen, *Metal Sci.* 16(1982)283.

[21] C. Zener, *J. Appl.* Phys. 20(1947)962.

[22] D. Murray and F. Landis, *Tans. ASME Ser.* 81D(1959). 106.

[23] R. A. Tanzilli and R. W. Heckel, *Trans. AIME* 242 (1968) 2313.

[24] N. J. W. Barker and A. Hellawell, *Metal Sci.* 8 (1974) 353.

[25] D. M. Goddard and W. J. Childs, *J. Less Common Metals* 58 (1978)217.